

New Randomized Global Generalized Minimum Residual (RGl-GMRES) method

A. Badahmane^a, Xian. Ming Gu^b

^a*The UM6P Vanguard Center, Mohammed VI Polytechnic University, Benguerir 43150, Lot 660, Hay Moulay Rachid, Morocco, email: badahmane.achraf@gmail.com*

^b*School of Mathematics, Southwestern University of Finance and Economics, Chengdu, Sichuan 611130, P.R. China, email: guxianming@live.cn*

Abstract

In this paper, we develop a new Randomized Global Generalized Minimum Residual (RGl-GMRES) algorithm for efficiently computing solutions to large-scale linear systems with multiple right-hand sides. The proposed method builds on a recently developed randomized global Gram–Schmidt process, in which sketched Frobenius inner products are employed to approximate the exact Frobenius inner products of high-dimensional matrices. We give some new convergence results of the randomized global GMRES method for multiple linear systems. In the case where the coefficient matrix A is diagonalizable, we derive new upper bounds for the randomized Frobenius norm of the residual. In this paper, we study how to introduce matrix sketching in this algorithm. It allows us to reduce the dimension of the problem in one of the main steps of the algorithm. To validate the effectiveness and practicality of this approach, we conduct several numerical experiments, which demonstrate that our RG-GMRES method is competitive with the Gl-GMRES method for solving large-scale problems with multiple right-hand sides.

Keywords: Randomized algorithms, Krylov subspace methods, GMRES

Notations. Let $\mathbb{R}^{n \times s}$ denote the space of real $n \times s$ matrices. For $Y, Z \in \mathbb{R}^{n \times s}$, we define the **Frobenius inner product** as

$$\langle Y, Z \rangle_F = \text{Trace}(Y^T Z).$$

The associated norm is the **Frobenius norm**, denoted by $\|\cdot\|_F$. A set of vectors (or matrices) in $\mathbb{R}^{n \times s}$ is said to be **F -orthonormal** if it is orthonormal with respect to the inner product $\langle \cdot, \cdot \rangle_F$. Finally, the **Kronecker product** of matrices C and D is defined as

$$C \otimes D = [c_{i,j}D],$$

where $c_{i,j}$ are the entries of C .

1. Introduction

The Randomized Global GMRES (RGl-GMRES) method is an iterative technique that incorporates randomization at different stages of the algorithm. Its principal advantage lies in the potential to significantly reduce computational costs, particularly those associated with the Frobenius inner product, which can be prohibitively expensive for large-scale matrices in deterministic global Krylov methods. By replacing exact Frobenius products with randomized estimators, RG1-GMRES achieves substantial efficiency gains while preserving strong theoretical guarantees and desirable convergence properties. The primary objective of this work is to develop a RG1-GMRES method for solving large-scale linear systems with multiple right-hand sides. Specifically, we consider linear systems with several right-hand sides of the form:

$$AX = B, \quad (1)$$

where A is an $n \times n$ large and sparse real matrix, and B and X are block vectors in $n \times s$, with $s \ll n$. Regarding B as a collection of columns b_i , $B := [b_1 | b_2 | \cdots | b_s]$ and also $X := [x_1 | x_2 | \cdots | x_s]$. One might consider applying methods for a single vector, such as those described in [1, 24], to each problem $Ax_i = b_i$, it is well known for linear systems. Instead of applying a standard iterative method to the solution of each one of the problems with several right-hand sides:

$$Ax_i = b_i, \quad i = 1, \dots, s, \quad (2)$$

independently, it is often more efficient to apply a global method to (2). However, that global Krylov approaches treating all columns b_i at once can be computationally advantageouss; see, e.g. [16, 8]. It is therefore reasonable to consider global version of GMRES for the solution of nonsymmetric problems with multiple right-hand sides (2). This version of GMRES has been introduced in [16] and studied in [8]. The method is based on the global version of the standard Arnoldi process; see, for example, [1]. In this work, we are particularly interested in the case where the number of right-hand sides s is very large, which makes standard Gl-GMRES subspace method computationally expensive due to the high cost of Frobenius inner products and orthogonalization procedures. This setting strongly motivates the use of randomized techniques, as they allow us to significantly reduce both computational and memory costs while retaining the essential convergence behavior of the Gl-GMRES framework. The paper is organized as follows. Section 2 is devoted to presenting the preliminary concepts and definitions of the Gl-GMRES method. The proposed randomized global algorithms outlined in Section 3. Section 4 reports numerical simulations for both the classical Gl-GMRES subspace method and its randomized variant. Finally, Section 5 provides recommendations for the use of randomized RG1-GMRES method based on the specific characteristics of the problem.

2. Global GMRES (Gl-GMRES) method

The global Krylov methods have been originally presented for solving a linear system of equations with multiple right-hand sides. It is well-known that the global Krylov subspace methods outperform other iterative methods for solving such systems when the coefficient matrix is large and nonsymmetric. On the other hand, the global Krylov subspace methods are also effective when applied for solving large and sparse linear matrix equations; for more details see In this section, we first briefly review the concept of the global GMRES method [5, 17] for solving large-scale linear systems with multiple right-hand sides. To begin, we will introduce some symbols and notations that will be referenced throughout this paper.

Definition 2.1. ([5, 17]). *Let \mathcal{X} and \mathcal{Y} are two matrices of dimension $n \times s$, we consider the scalar product*

$$\langle \mathcal{X}, \mathcal{Y} \rangle_F = \text{Trace}(\mathcal{X}^T \mathcal{Y}), \quad (3)$$

where *Trace* is the trace of the square matrix $\mathcal{X}^T \mathcal{Y}$, refers to the sum of its diagonal entries. The associated norm is the Frobenius norm, denoted $\|\cdot\|_F$, which can be expressed as follows:

$$\|\mathcal{X}\|_F = \sqrt{\text{Trace}(\mathcal{X}^T \mathcal{X})}. \quad (4)$$

Definition 2.2. *Let $V \in \mathbb{R}^{n \times s}$, the global Krylov subspace $\mathcal{K}_k(A, V)$ is the subspace spanned by the matrices $V, AV, \dots, A^{k-1}V$.*

Remark 2.1. *Let V be a real matrix of dimension $n \times s$. According to the definition of the subspace $\mathcal{K}_k(A, V)$, we have*

$$\mathcal{Z} \in \mathcal{K}_k(A, V) \iff \mathcal{Z} = \sum_{i=1}^k \psi_i A^{i-1} V, \quad \psi_i \in \mathbb{R}, i = 1, \dots, k.$$

In other words, $\mathcal{K}_k(A, V)$ is the subspace of $\mathbb{R}^{n \times s}$ that contains all the matrices of dimension $n \times s$, written as $\mathcal{Z} = \Theta(A)V$, where Θ is a polynomial of degree at most equal $k - 1$.

Definition 2.3. *The Kronecker product of M and J , where M is a matrix with dimension $m \times r$ and J is a matrix with dimensions $n \times s$, can be expressed in a specific mathematical form*

$$M \otimes J = \begin{pmatrix} M_{11}J & \dots & M_{1r}J \\ \vdots & \ddots & \vdots \\ M_{m1}J & \dots & M_{mr}J \end{pmatrix} \in \mathbb{R}^{mn \times rs}. \quad (5)$$

Definition 2.4. (Diamond Product) Let Y and \mathcal{Z} be matrices of dimensions $n_u \times ls$ and $n_u \times lr$, respectively. The matrices Y and \mathcal{Z} are constructed by concatenating $n_u \times l$ matrices Y_i and \mathcal{Z}_j (for $i = 1, \dots, s$ and $j = 1, \dots, r$). The symbol \diamond represents a specific product defined by the following formula:

$$Y^T \diamond \mathcal{Z} = \begin{pmatrix} \langle Y_1, \mathcal{Z}_1 \rangle_F & \langle Y_1, \mathcal{Z}_2 \rangle_F & \dots & \langle Y_1, \mathcal{Z}_r \rangle_F \\ \langle Y_2, \mathcal{Z}_1 \rangle_F & \langle Y_2, \mathcal{Z}_2 \rangle_F & \dots & \langle Y_2, \mathcal{Z}_r \rangle_F \\ \vdots & \vdots & \ddots & \vdots \\ \langle Y_s, \mathcal{Z}_1 \rangle_F & \langle Y_s, \mathcal{Z}_2 \rangle_F & \dots & \langle Y_s, \mathcal{Z}_r \rangle_F \end{pmatrix} \in \mathbb{R}^{s \times r}.$$

We use the global Arnoldi process for building an F -orthonormal basis of $\mathcal{K}_k(A, V)$. Let X_0 be the initial approximate solution of

$$AX = B, \quad (1.1)$$

and let $R_0 = B - AX_0$ be the corresponding residual.

2.1. Gl-Arnoldi method

The following global Arnoldi process, which is based on the modified Gram–Schmidt process, constructs an F -orthonormal basis V_1, V_2, \dots, V_k of $\mathcal{K}_k(A, R_0)$. In other words,

$$\text{Trace}(V_i^T V_j) = \delta_{ij}, \quad i, j = 1, \dots, k, \quad (6)$$

where δ_{ij} is the Kronecker symbol.

Algorithm 1 Gl-Arnoldi process

```

1:  $V_1 = R_0 / \|R_0\|_F$ 
2: for  $j = 1, 2, \dots, k$  do
3:    $W := AV_j$ 
4:   for  $i = 1, 2, \dots, j$  do
5:      $h_{i,j} = \langle W, V_i \rangle_F$ 
6:      $W = W - h_{i,j} V_i$ 
7:   end for
8:    $h_{j+1,j} = \|W\|_F$ 
9:    $V_{j+1} = W / h_{j+1,j}$ 
10: end for

```

Proposition 1. Assume that $h_{i+1,i} \neq 0$ for $i = 1, \dots, k$, and let

$$\mathcal{V}_k = [V_1, V_2, \dots, V_k],$$

where V_i , for $i = 1, \dots, k$, are the matrices computed by Algorithm 1. Then the following relations hold:

$$\begin{aligned} A\mathcal{V}_k &= \mathcal{V}_k \diamond H_k + h_{k+1,k}[O, \dots, O, V_{k+1}], \\ A\mathcal{V}_k &= \mathcal{V}_{k+1} \diamond \bar{H}_k, \end{aligned} \quad (7)$$

where $H_k \in \mathbb{R}^{k \times k}$ is an upper Hessenberg matrix and $\tilde{V}_k = [V_1, \dots, V_{k+1}]$.

$$\mathcal{V}_{k+1} = [V_1, \dots, V_k, V_{k+1}] \in \mathbb{R}^{n \times (k+1)s}, \quad \bar{H}_k \in \mathbb{R}^{(k+1) \times k}.$$

The global GMRES method constructs, at step k , the approximation X_k satisfying the following two relations:

$$X_k - X_0 \in \mathcal{K}_k(A, R_0), \quad \langle A^j R_0, R_k \rangle_F = 0, \quad j = 1, \dots, k. \quad (8)$$

The residual $R_k = B - AX_k$ satisfies the minimization property

$$\|R_k\|_F = \min_{Z \in \mathcal{K}_k(A, R_0)} \|R_0 - AZ\|_F. \quad (4.1)$$

Problem (4.1) is solved by applying the global Arnoldi process.

2.2. Convergence analysis of the Gl-GMRES method

In this section, we recall a bound for the residual R_k in (4.1). Let

$$A = ZDZ^{-1},$$

where D is the diagonal matrix whose elements are the eigenvalues $\lambda_1, \dots, \lambda_{n+m}$, and Z is the eigenvector matrix.

Theorem 2.1. [8]. Let the initial residual be decomposed as

$$R_0 = Z\beta,$$

where β is an $(n+m) \times s$ matrix whose columns are denoted by $\beta^{(1)}, \dots, \beta^{(s)}$. Let $R_k = B - AX_k$ be the k th residual obtained by the global GMRES method applied to (1.1). Then

$$\|R_k\|_F^2 \leq \frac{\|Z\|_2^2}{e_1^T (V_{k+1}^T D V_{k+1})^{-1} e_1}, \quad (9)$$

where

$$D = \begin{bmatrix} \sum_{i=1}^s |\beta_1^{(i)}|^2 & & \\ & \ddots & \\ & & \sum_{i=1}^s |\beta_{n+m}^{(i)}|^2 \end{bmatrix}.$$

and

$$V_{k+1} = \begin{bmatrix} 1 & \lambda_1 & \cdots & \lambda_1^k \\ \vdots & \vdots & & \vdots \\ 1 & \lambda_{n+m} & \cdots & \lambda_{n+m}^k \end{bmatrix}.$$

The coefficients $\beta_1^{(i)}, \dots, \beta_{n+m}^{(i)}$ are the components of the vector $\beta^{(i)}$, and e_1 is the first unit vector of \mathbb{R}^{k+1} .

Algorithm 2 Gl-GMRES algorithm

1: Initialize **Require**:

$$A \in \mathbb{R}^{n \times n}, \quad B \in \mathbb{R}^{n \times s},$$

2: **for** $j = 1, 2, \dots, k$ **do**
 3: $W := AV_j$
 4: **for** $i = 1, 2, \dots, j$ **do**
 5: $h_{i,j} = \langle W, V_i \rangle_F$
 6: $W = W - h_{i,j}V_i$
 7: **end for**
 8: $h_{j+1,j} = \|W\|_F$
 9: $V_{j+1} = W/h_{j+1,j}$
 10: **end for**

11: Solve the least square problem:

$$H_{k+1,k}z = \beta e_1,$$

12: Set

$$X_k = X_0 + V_k \diamond z, \quad R_k = B - AX_k$$

3. RGl-GMRES method

Global Krylov subspace methods have been widely studied and used for solving large-scale linear systems and inverse problems with multiple right-hand sides, including saddle point problems arising in constrained optimization, fluid dynamics, and mixed finite element discretizations. In these methods, each iteration typically requires one or more matrix–block–vector products with the saddle point operator \mathbf{A} . Considerable effort has been devoted to reducing the cost of these products, for example by exploiting problem structure, sparsity, or fast operator implementations. Despite these advances, the computational cost of orthonormalization of block vectors remains a major challenge in global Krylov subspace methods. In particular, the computation of Frobenius inner products between matrix-valued basis elements can be expensive when the underlying

problem dimension is large or when many Krylov iterations are required. Randomized techniques have recently been introduced into Krylov subspace methods to alleviate the cost of orthonormalization; see, for instance, [26, 22]. Most of these approaches rely on random sketching to approximate inner products at reduced computational and communication cost.

3.1. Introduction to random sketching

Let $\Theta \in \mathbb{R}^{\ell \times n}$, with $\ell \ll n$, be a sketching matrix. This matrix can be viewed as an embedding of subspaces of \mathbb{R}^n into subspaces of \mathbb{R}^ℓ and is therefore referred to as an ℓ_2 -subspace embedding. The ℓ_2 inner products between vectors in subspaces of \mathbb{R}^n are approximated by

$$\langle \cdot, \cdot \rangle \approx \langle \Theta \cdot, \Theta \cdot \rangle.$$

For a given (low-dimensional) subspace of interest $\mathcal{V} \subset \mathbb{R}^n$, the quality of this approximation can be characterized by the following property of Θ :

Definition 3.1 (Subspace embedding). *Let $\varepsilon < 1$, and let $\Theta \in \mathbb{R}^{\ell \times n}$ be a sketching matrix. The matrix Θ is said to be an ε -subspace embedding for a subspace $\mathcal{V} \subset \mathbb{R}^n$ if*

$$\forall x, y \in \mathcal{V}, \quad |\langle x, y \rangle - \langle \Theta x, \Theta y \rangle| \leq \varepsilon \|x\|_2 \|y\|_2. \quad (10)$$

Let $V \in \mathbb{R}^{n \times \ell}$ be a matrix whose columns form a basis of \mathcal{V} . For ease of presentation in the following sections, an ε -subspace embedding for \mathcal{V} will often be referred to simply as an ε -embedding for V .

Proposition 2. *If $\Theta \in \mathbb{R}^{\ell \times n}$ is an ε -embedding for V , then the singular values of V satisfy*

$$(1 + \varepsilon)^{-1/2} \sigma_{\min}(\Theta V) \leq \sigma_{\min}(V) \leq \sigma_{\max}(V) \leq (1 - \varepsilon)^{-1/2} \sigma_{\max}(\Theta V). \quad (11)$$

We now extend the above results from vector spaces to matrix spaces by using the Frobenius inner product

Definition 3.2 (Subspace embedding). *Let $\varepsilon < 1$, and let $\Theta \in \mathbb{R}^{\ell \times n}$ be a sketching matrix. The matrix Θ is said to be an ε -subspace embedding for a subspace $\mathcal{V} \subset \mathbb{R}^n$, if $\forall x_i, y_i \in \mathcal{V}$, where $X = [x_1, \dots, x_s]$ and $Y = [y_1, \dots, y_s]$, then*

$$|\langle X, Y \rangle - \langle \Theta X, \Theta Y \rangle| \leq \varepsilon \|X\|_F \|Y\|_F. \quad (12)$$

Proof. Let $X = [x_1, \dots, x_s] \in \mathbb{R}^{d \times s}$ and $Y = [y_1, \dots, y_s] \in \mathbb{R}^{d \times s}$ be arbitrary. Then

By using Definition 3.1

$$x_i, y_i \in \mathcal{V}, \quad |\langle x_i, y_i \rangle - \langle \Theta x_i, \Theta y_i \rangle| \leq \varepsilon \|x_i\|_2 \|y_i\|_2. \quad (13)$$

Summing over all s columns, we get

$$|\langle X, Y \rangle - \langle \Theta X, \Theta Y \rangle| \leq \varepsilon \|X\|_F \|Y\|_F. \quad (14)$$

□

Definition 3.3 (Matrix Subspace Embedding). *Let $V \in \mathbb{R}^{n \times \ell}$ have full column rank, and let*

$$\mathcal{U} = \{VX \in \mathbb{R}^{n \times s} : X \in \mathbb{R}^{\ell \times s}\}.$$

A matrix $\Theta \in \mathbb{R}^{d \times n}$ is called an ε -subspace embedding for \mathcal{U} if, for all $X \in \mathbb{R}^{\ell \times s}$,

$$(1 + \varepsilon)^{-1} \|\Theta VX\|_F^2 \leq \|VX\|_F^2 \leq (1 - \varepsilon)^{-1} \|\Theta VX\|_F^2, \quad (15)$$

where $\|\cdot\|_F$ denotes the Frobenius norm.

Proposition 3 (Matrix embedding from vector embedding). *If Θ is an ε -subspace embedding for the vector subspace $\text{range}(V) \subset \mathbb{R}^n$, then it is also an ε -subspace embedding for the matrix subspace*

$$\mathcal{U} = \{VX : X \in \mathbb{R}^{\ell \times s}\} \subset \mathbb{R}^{n \times s}.$$

Proof. Let $X = [x_1, \dots, x_s] \in \mathbb{R}^{\ell \times s}$ be arbitrary. Then by assumption, Θ is an ε -embedding for $\text{range}(V)$, so for each column x_j ,

$$(1 + \varepsilon) \|\Theta V x_j\|_2^2 \leq \|V x_j\|_2^2 \leq (1 - \varepsilon) \|\Theta V x_j\|_2^2.$$

Summing over all s columns, we get

$$(1 + \varepsilon) \sum_{j=1}^s \|\Theta V x_j\|_2^2 \leq \sum_{j=1}^s \|V x_j\|_2^2 \leq (1 - \varepsilon) \sum_{j=1}^s \|\Theta V x_j\|_2^2,$$

which is equivalent to

$$(1 + \varepsilon) \|\Theta VX\|_F^2 \leq \|VX\|_F^2 \leq (1 - \varepsilon) \|\Theta VX\|_F^2.$$

Since X was arbitrary, this proves that Θ is an ε -embedding for the matrix subspace \mathcal{U} . \square

Definition 3.4 (Matrix Subspace Embedding). *Let $V \in \mathbb{R}^{n \times d}$ have full column rank, and let*

$$\mathcal{U} = \{VX \in \mathbb{R}^{n \times s} : X \in \mathbb{R}^{\ell \times s}\}.$$

A matrix $\Theta \in \mathbb{R}^{d \times n}$ is called an ε -subspace embedding for \mathcal{U} if, for all $X \in \mathbb{R}^{\ell \times s}$,

$$(1 - \varepsilon) \|VX\|_F^2 \leq \|\Theta VX\|_F^2 \leq (1 + \varepsilon) \|VX\|_F^2, \quad (16)$$

where $\|\cdot\|_F$ denotes the Frobenius norm.

Proposition 4 (Singular-value bounds for matrix subspace embeddings). *If Θ is an ε -subspace embedding for \mathcal{U} , then for any matrix $X \in \mathbb{R}^{\ell \times s}$,*

$$(1 + \varepsilon)^{-1/2} \sigma_{\min}(\Theta VX) \leq \sigma_{\min}(VX) \leq \sigma_{\max}(VX) \leq (1 - \varepsilon)^{-1/2} \sigma_{\max}(\Theta VX), \quad (17)$$

where $\sigma_{\min}(\cdot)$ and $\sigma_{\max}(\cdot)$ denote the minimal and maximal singular values of the matrix.

Proof. Let $X \in \mathbb{R}^{\ell \times s}$ be arbitrary. By the Frobenius-norm subspace embedding, we have

$$(1 - \varepsilon) \|\Theta V X\|_F^2 \leq \|V X\|_F^2 \leq (1 + \varepsilon) \|\Theta V X\|_F^2.$$

Which can be rewritten as follows:

$$(1 + \varepsilon) \sum_{j=1}^s \|\Theta V x_j\|_2^2 \leq \sum_{j=1}^s \|V x_j\|_2^2 \leq (1 - \varepsilon) \sum_{j=1}^s \|\Theta V x_j\|_2^2, \quad (18)$$

and we will divide (18) by x_j ,

$$(1 + \varepsilon) \sum_{j=1}^s \frac{\|\Theta V x_j\|_2^2}{\|x_j\|_2^2} \leq \sum_{j=1}^s \frac{\|V x_j\|_2^2}{\|x_j\|_2^2} \leq (1 - \varepsilon) \frac{\sum_{j=1}^s \|\Theta V x_j\|_2^2}{\sum_{j=1}^s \|x_j\|_2^2}, \quad (19)$$

$$(1 + \varepsilon) \sum_{j=1}^s \frac{\|\Theta V x_j\|_2^2}{\|x_j\|_2^2} \leq \sum_{j=1}^s \frac{\|V x_j\|_2^2}{\|x_j\|_2^2} \leq (1 - \varepsilon) \sum_{j=1}^s \frac{\|\Theta V x_j\|_2^2}{\|x_j\|_2^2}, \quad (20)$$

$$(1 + \varepsilon) s \sigma_{\min}(\Theta V) \leq (1 + \varepsilon) \sum_{j=1}^s \frac{\|\Theta V x_j\|_2^2}{\|x_j\|_2^2}, \quad (21)$$

$$s \sigma_{\min}(V) \leq \sum_{j=1}^s \frac{\|V x_j\|_2^2}{\|x_j\|_2^2} \leq s \sigma_{\max}(V) \leq (1 - \varepsilon) \sum_{j=1}^s \frac{\|\Theta V x_j\|_2^2}{\|x_j\|_2^2} \leq (1 - \varepsilon) s \sigma_{\max}(\Theta V), \quad (22)$$

By using (18), (19) and (22), we conclude that:

$$(1 + \varepsilon)^{-1/2} \sigma_{\min}(\Theta V X) \leq \sigma_{\min}(V X) \leq \sigma_{\max}(V X) \leq (1 - \varepsilon)^{-1/2} \sigma_{\max}(\Theta V X), \quad (23)$$

since X was arbitrary, this proves the proposition. \square

3.2. Randomized Global Arnoldi (RGl-Arnoldi) method

At the k th iteration of the Gl-GMRES method, the solution to (2) can be approximated by:

$$X_k = \mathcal{V}_{k+1} \diamond z_k, \quad \text{where } z_k = \operatorname{argmin}_z \|\beta e_1 - \bar{H}_k z\| \quad \text{with } \beta = \|B\|_F. \quad (24)$$

Here and in the following, e_1 denotes the 1-th canonical basis vector, whose size should be clear from the context. Note that the orthonormalization process can be costly for very large dimensional blocks. One remedy to mitigate the computational cost of the global Gram-Schmidt (Gl-Gram-Schmidt) process is to use the RGl-Gram-Schmidt process that exploits sketching, as described in [2].

Before defining the RGl-Arnoldi, we will introduce some symbols and notations that will be used for this method.

Definition 3.5. Let \mathcal{X} and \mathcal{Y} are two matrices of dimension $n \times s$, we consider the sketched inner product

$$\langle \mathcal{X}, \mathcal{Y} \rangle_{\Theta} = \text{Trace}(\mathcal{X}^T \Theta^T \Theta \mathcal{Y}). \quad (25)$$

The RGl-Arnoldi approach is obtained by applying the randomized Gl-Gram-Schmidt algorithm to the global Krylov subspace $\mathcal{K}_k(A, B)$. More precisely, after k iterations of RGl-Arnoldi, we have a basis $\{Q_1, \dots, Q_{k+1}\}$ of $\mathcal{K}_{k+1}(A, B)$ with blocks Q_i , $i = 1, \dots, k+1$, that are orthonormal with respect to the sketched inner product (25), and an upper Hessenberg matrix $\bar{E}_k \in \mathbb{R}^{(k+1) \times k}$. Let $\mathcal{Q}_k = [Q_1, \dots, Q_k] \in \mathbb{R}^{n \times ks}$ and $\mathcal{Q}_{k+1} = [\mathcal{Q}_k, Q_{k+1}] \in \mathbb{R}^{n \times (k+1)s}$, then we get a RGl-Arnoldi method identity analogous to Gl-Arnoldi method (see Section 2.1)

$$A\mathcal{Q}_k = \mathcal{Q}_{k+1}\bar{E}_k. \quad (26)$$

Algorithm summarizes the main steps involved in the new RGl-Arnoldi algorithm Build-

Algorithm 3 The RGl-Arnoldi process

```

1: Initialize  $\tilde{Q}_1 = R_0$ .
2: Sketch  $\tilde{S}_1 = \Theta R_0$ .
3: Compute the sketched (semi) norm  $\beta = \|\tilde{S}_1\|_F$ .
4: Scale blocks  $S_1 = \tilde{S}_1/\beta$  and  $Q_1 = \tilde{Q}_1/\beta$ .
5: for  $j = 1, 2, \dots, k$  do
6:    $W := A\mathcal{Q}_j$ 
7:    $Z := \Theta W$ 
8:   for  $i = 1, 2, \dots, j$  do
9:      $E_{i,j} = \langle W, Q_i \rangle_{\Theta} = \langle \Theta W, \Theta Q_i \rangle_F$ 
10:     $W = W - E_{i,j}Q_i$ 
11:     $Z = Z - E_{i,j}Q_i$ 
12:   end for
13:    $E_{j+1,j} = \|Z\|_F$ 
14:    $Q_{j+1} = W/E_{j+1,j}$  and  $S_{j+1} = Z/E_{j+1,j}$ .
15: end for

```

ing on the RGl-Arnoldi algorithm, the RGl-GMRES solution at the k th iteration is given by:

$$X_k^r = \mathcal{Q}_k \diamond z_k^r \quad \text{where} \quad z_k^r = \text{argmin}_z \|E_k z - \beta e_1\| \quad \text{and} \quad \beta = \|\Theta B\|. \quad (27)$$

The k th RGl-GMRES approximation X_k^r minimizes the sketched (semi)norm of the residual over $\mathcal{K}_k(A, B)$, since

$$\|E_k z_k^r - \beta e_1\| = \min_z \|E_k z - \beta e_1\| = \min_z \|\Theta \mathcal{Q}_{k+1} \diamond (E_k z - \beta e_1)\|_F \quad (28)$$

$$= \min_z \|\Theta(A\mathcal{Q}_k \diamond z - B)\| = \|\Theta(AX_k^r - B)\|_F. \quad (29)$$

Definition 3.6. *This optimality property of RGl-GMRES can be also derived from more general facts about projection methods (as described, for instance, in [23] indeed, the k th RGl-GMRES approximation is such that*

$$X_k^r \in \mathcal{K}_k(A, B) \quad \text{and} \quad R_k \perp_{\langle \Theta \cdot, \Theta \cdot \rangle_F} A\mathcal{K}_k(A, B),$$

where, by \perp_{Θ} , we mean orthogonal with respect to the sketched inner product $\langle \Theta \cdot, \Theta \cdot \rangle_F$.

Note that the above properties generalize to those used by standard GMRES, which would hold with $\Theta = I_n$.

Proposition 5. *Assume that Θ is an $(\epsilon, \delta, K + 1)$ -oblivious embedding, Then we have the following bound for the RGl-GMRES residual $B - AX_k$ norm with respect to the GMRES residual $B - AX_k$ norm at the k th iteration*

$$\|B - AX_k^r\|_F^2 \leq \frac{(1 + \epsilon)}{(1 - \epsilon)} \|B - AX_k\|_F^2.$$

Proof. Standard Gl-GMRES (unsketched)

The k -th Gl-GMRES iterate X_k is defined as:

$$X_k = \arg \min_{X \in X_0 + \mathcal{K}_k(A, B)} \|B - AX\|_F. \quad (30)$$

That is, Gl-GMRES method minimizes the true residual norm over the affine Krylov subspace. The k -th RGl-GMRES iterate X_k^r is defined as :

$$X_k^r = \arg \min_{X \in X_0 + \mathcal{K}_k(A, B)} \|\Theta(B - AX)\|_F. \quad (31)$$

That is, RGl-GMRES minimizes the sketched residual norm over the same affine Krylov subspace. Since Θ is an $(\epsilon, \delta, k + 1)$ -subspace embedding and by using Definition 3.4, we get

$$(1 - \epsilon) \|B - AX_k^r\|^2 \leq \|\Theta(B - AX_k^r)\|_F^2,$$

using the RGl-GMRES optimality (31) and inequality (32)

$$\|\Theta(B - AX_k^r)\|_F^2 \leq \|\Theta(B - AX_k)\|_F^2 \leq (1 + \epsilon) \|B - AX_k\|_F^2.$$

□

Theorem 3.1. [8]. *Let the initial residual be decomposed as*

$$R_0 = Z\beta,$$

where β is an $(n+m) \times s$ matrix whose columns are denoted by $\beta^{(1)}, \dots, \beta^{(s)}$. Let $R_k = B - AX_k$ be the k th residual obtained by the RGl-GMRES method applied to (2). Then

$$\|B - AX_k^r\|_F^2 \leq \Gamma \frac{\|Z\|_2^2}{e_1^T (V_{k+1}^T DV_{k+1})^{-1} e_1}, \quad (32)$$

where

$$D = \begin{bmatrix} \sum_{i=1}^s |\beta_1^{(i)}|^2 & & & \\ & \ddots & & \\ & & \ddots & \\ & & & \sum_{i=1}^s |\beta_{n+m}^{(i)}|^2 \end{bmatrix}.$$

and

$$V_{k+1} = \begin{bmatrix} 1 & \lambda_1 & \dots & \lambda_1^k \\ \vdots & \vdots & & \vdots \\ 1 & \lambda_{n+m} & \dots & \lambda_{n+m}^k \end{bmatrix}.$$

The coefficients $\beta_1^{(i)}, \dots, \beta_{n+m}^{(i)}$ are the components of the vector $\beta^{(i)}$, and e_1 is the first unit vector of \mathbb{R}^{k+1} and $\Gamma > 0$.

Proof. By Theorem 2.1, the k th residual generated by the RGl-GMRES method satisfies

$$\|B - AX_k\|_F^2 \leq \frac{\|Z\|_2^2}{e_1^T (V_{k+1}^T DV_{k+1})^{-1} e_1}, \quad (33)$$

Furthermore, Proposition 5 implies that

$$\|B - AX_k^r\|_F^2 \leq \Gamma \frac{\|Z\|_2^2}{e_1^T (V_{k+1}^T DV_{k+1})^{-1} e_1}, \quad (34)$$

defining $\Gamma = \frac{(1+\epsilon)}{(1-\epsilon)}$, completes the proof. \square

Based on the above analysis, we now present the RGl-GMRES algorithm for large-scale linear systems with multiple right-hand sides problems

4. Numerical Results

This section presents numerical examples to illustrate the effectiveness of the RGl-GMRES and Gl-GMRES algorithms for solving (2). The initial matrix X_0 is set to be a random matrix. When solving systems with multiple right-hand sides (2) in Algorithms 2 and 3. The norm of the relative residual is lower than the given tolerance ($tol = 10^{-6}$). In the sense of the following terms:

- ℓ : denotes the sketch size,

Algorithm 4 The RGl-GMRES algorithm

1: **Require:**

$$A \in \mathbb{R}^{n \times n}, \quad B \in \mathbb{R}^{n \times s}, \quad \Theta \in \mathbb{R}^{\ell \times n}, \quad \ell \ll n$$

2: Initialize $\tilde{V}_1 = R_0$.

3: Sketch $\tilde{S}_1 = \Theta R_0$.

4: Compute the sketched (semi) norm $\beta = \|\tilde{S}_1\|$.

5: Scale blocks $V_1 = \tilde{V}_1/\beta$ and $S_1 = \tilde{S}_1/\beta$.

6: **for** $j = 1, 2, \dots, k$ **do**

7: $W := AV_j$.

8: Sketch $Z = \Theta W$.

9: **for** $i = 1, 2, \dots, j$ **do**

10: $h_{i,j} = \langle W, V_i \rangle_\Theta = \langle \Theta W, \Theta V_i \rangle_F$.

11: $W = W - h_{i,j} V_i$.

12: $Z = Z - h_{i,j} S_i$.

13: **end for**

14: Compute the sketched (semi)norm $h_{j+1,j} = \|S\|_F$.

15: Scale blocks: $V_{j+1} = W/h_{j+1,j}$ and $S_{j+1} = S_{j+1}/h_{j+1,j}$.

16: **end for**

17: Solve the randomized least square problem:

$$H_{k+1,k} z = \beta e_1,$$

18: Set

$$X_k = X_0 + V_k \diamond z, \quad R_k = B - AX_k.$$

- CPU: denotes the elapsed CPU time of the convergence in (seconds),
- Iter_{Gl-GMRES}: number of iterations of Gl-GMRES method,
- Iter_{RGl-GMRES}: number of iterations of randomized Gl-GMRES method,
- Res: norm of absolute relative residual is defined as :

$$\text{Res} = \|B - AX^{(k)}\|_F,$$

- RES: norm of absolute error is given as follows:

$$\text{ERR} = \|X^* - X^{(k)}\|_F,$$

where: $X^{(k)}$ is the approximate solution of (2). In addition, we have used right-hand sides corresponding to random solution vectors. In Table 1 for various problem sizes, we report the number of iterations (IT), CPU times, residual (RES) and error (ERR) of the tested Gl-GMRES and RGl-GMRES methods, with respect to different values of sketch size ℓ .

Navier-Stokes model: Lid-driven cavity

Example 1. *Square domain Ω_{\square} , enclosed flow boundary condition. Let us consider the system of Navier-Stokes equations in [12], posed on two-dimensional domain $\Omega_{\square} = (-1, 1) \times (-1, 1)$. In this particular case, we consider a flow in square cavity with the lid moving from left to right. This configuration we are referring to is widely recognized as a "leaky two-dimensional lid-driven cavity (with $u_x = 1$, is the horizontal velocity on the lid)". Dirichlet no-flow boundary conditions are taken on the side and bottom of domain on uniform streamline. We use $Q_2 - P_1$ mixed-finite element approximation from IFISS library [12] to discretize this problem in Ω_{\square} , where*

- Q_2 : biquadratic finite element approximation on rectangles for the velocity,
- P_1 : triangular finite element approximation on triangle for the pressure,

the nodal positions of this mixed-finite element are illustrated in the following Fig. 1:

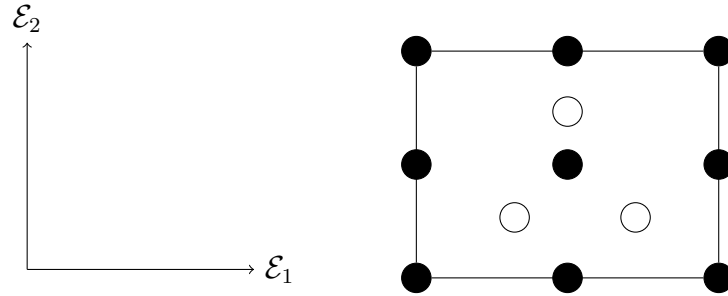


Figure 1:

$Q_2 - P_1$ element (● velocity node; ○ pressure node), local co-ordinate $(\mathcal{E}_1, \mathcal{E}_2)$.

We then obtain the matrix A of the linear systems (refer to equation 2). To generate the linear systems corresponding to different refinement levels, specifically for levels $l = 4, 5, 6, 7$, and 8 , we utilize the IFISS software package developed by Elman et al. [12], which provides the matrix A for the lid-driven cavity problem. Table 1 summarizes general information about the test problems, including the dimension n . In the following numerical results, we set the viscosity to $\nu = 1/100$.^a

Table 1: The size of the matrix A

Lid driven cavity ¹		
l	n	size of A
4	578	578×578
5	2178	2178×2178
6	8450	8450×8450
7	33282	33282×33282
8	132098	132098×132098

^aLid driven cavity.

A comparison of the Gl-GMRES and RGl-GMRES methods for solving the linear system (2) of size $n = 33,282$ with $s = 10$ right-hand sides is presented in Table 2. Performance is evaluated in terms of computational time (CPU), number of iterations (Iter), and final residual norm (Res).

Table 2: Results of the Gl-GMRES and RGl-GMRES methods with $l = 7$ and $s = 10$.

Method	ℓ	CPU(s)	Iter	Res
Gl-GMRES	—	11.210	749	1.15×10^{-6}
RGl-GMRES	20	14.134	1193	1.62×10^{-5}
RGl-GMRES	50	9.675	860	2.68×10^{-6}
RGl-GMRES	80	8.952	787	1.85×10^{-6}

The results demonstrate that the performance of RGl-GMRES depends strongly on the sketch size ℓ . For a small sketch size ($\ell = 20$), RGl-GMRES requires more iterations and a higher computational cost than standard Gl-GMRES. However, increasing the sketch size improves both efficiency and accuracy: with $\ell = 50$ and $\ell = 80$, RGl-GMRES achieves lower CPU times while delivering residual norms comparable to those of Gl-GMRES. These findings indicate that with a suitably chosen sketch size, RGl-GMRES can outperform classical Gl-GMRES for large-scale problems without sacrificing accuracy. We next consider the same problem but with a much larger number of right-hand sides, $s = 400$. The corresponding results are shown in Table 3.

Table 3: Results of the Gl-GMRES and RGl-GMRES methods with $l = 7$ and $s = 400$.

Method	ℓ	CPU(s)	Iter	Res
Gl-GMRES	—	43.569	47	7.75×10^{-8}
RGl-GMRES	30	22.97	46	7.28×10^{-8}
RGl-GMRES	60	22.60	47	5.55×10^{-8}
RGl-GMRES	100	20.59	47	6.17×10^{-8}

The results clearly show that with $s = 400$, RGl-GMRES significantly outperforms the standard Gl-GMRES method in terms of computational efficiency, reducing the CPU time by nearly 50 % for all tested sketch sizes while maintaining comparable iteration counts and residual norms. Comparing the results from Table 2 ($s = 10$) and Table 3 ($s = 400$), we observe that increasing the number of right-hand sides amplifies the advantages of the randomized approach. For a moderate number of right-hand sides ($s = 10$), RGl-GMRES only becomes competitive when the sketch size is chosen sufficiently large (e.g., $\ell \geq 50$). In contrast, with a large number of right-hand sides ($s = 400$), even a modest sketch size (e.g., $\ell = 30$) yields a substantial speedup. This trend highlights the scalability of RGl-GMRES: the cost savings from sketching become more pronounced as the number of right-hand sides increases, making the randomized method particularly effective for large-scale systems with multiple right-hand sides.

In Table 4, we list the CPU times of Gl-GMRES and RGl-GMRES methods for solving (2).

Table 4: Results of the Gl-GMRES and RGl-GMRES methods with $l = 7$ and $s = 700$

Method	ℓ	CPU(s)	Iter	Res
Gl-GMRES	–	678.419	47	5.85×10^{-8}
RGl-GMRES	30	361.996	47	5.83×10^{-8}
RGl-GMRES	60	393.597	47	5.41×10^{-8}
RGl-GMRES	100	393.203	47	5.90×10^{-8}

The results in Table 4, for $s = 700$ right-hand sides, further confirm the scalability advantage of RGl-GMRES method. For this large-scale problem, all methods converge in the same number of iterations (47) and achieve comparable residual norms ($\sim 5 \times 10^{-8}$). However, RGl-GMRES method provides substantial computational savings: with $d = 30$, the CPU time is reduced by nearly 47 % compared to standard Gl-GMRES. Interestingly, increasing the sketch size beyond $d = 30$ yields diminishing returns in this case, as the overhead of a larger sketch offsets additional computational benefits. This pattern suggests that the optimal sketch size may depend on both the number of right-hand sides and the problem size, but even modest sketch sizes can provide dramatic speedups for large s . Overall, the progression from $s = 10$ (Table 2) to $s = 400$ (Table 3) to $s = 700$ (Table 4) demonstrates that the efficiency gains of RGl-GMRES method become increasingly significant as the number of right-hand sides grows. This highlights the method’s strong potential for large-scale applications involving multiple right-hand sides.

Table 5: Results of the Gl-GMRES and RGl-GMRES methods with $l = 7$ and $s = 900$

Method	ℓ	CPU Time (s)	Iter	Res
Gl-GMRES	–	1129.079	47	5.16×10^{-8}
RGl-GMRES	$\ell = 30$	740.324	47	5.34×10^{-8}
RGl-GMRES	$\ell = 60$	823.003	47	5.28×10^{-8}
RGl-GMRES	$\ell = 100$	749.796	47	5.16×10^{-8}

Table 5 presents results for the largest tested number of right-hand sides, $s = 900$. The pattern observed in previous tables continues: all methods converge in 47 iterations with nearly identical residual norms ($\sim 5 \times 10^{-8}$). The computational advantage of RGl-GMRES remains substantial, achieving approximately 34-35 % reduction in CPU time with $\ell = 30$ and $\ell = 100$ compared to standard Gl-GMRES. When viewed alongside results for $s = 10$, $s = 400$, and $s = 700$, a clear trend emerges: the relative efficiency gain of RGl-GMRES increases with the number of right-hand sides. While for $s = 10$ the method only became competitive with sufficiently large ℓ , for $s = 900$ even modest sketch sizes yield significant speedups. This demonstrates the strong scalability of randomized sketching for problems with many right-hand sides, where the cost reduction from dimensionality reduction outweighs the overhead of sketching operations.

The consistent iteration counts across all methods further confirm that randomization preserves convergence behavior while dramatically improving computational efficiency.

Table 6: Results of the Gl-GMRES vs RGl-GMRES methods, with $l = 8$ and $s = 400$

Method	Parameter	CPU Time (s)	Iterations	Final Residual
Gl-GMRES	—	3588.648	49	1.36×10^{-5}
RGl-GMRES	$\ell = 30$	2413.264	50	9.62×10^{-6}
RGl-GMRES	$\ell = 60$	2081.544	49	1.37×10^{-5}
RGl-GMRES	$\ell = 100$	1968.227	50	9.46×10^{-6}

Table 6 presents results for an even larger problem with $l = 8$ (approximately $91,138 \times 91,138$) and $s = 400$ right-hand sides. This demonstrates the scalability of RGl-GMRES to higher-dimensional systems. While the absolute CPU times increase significantly due to the larger problem size, the performance advantage of RGl-GMRES remains clear. With sketch sizes $\ell = 60$ and $\ell = 100$, RGl-GMRES achieves 42-45 % reductions in computational time compared to standard Gl-GMRES, while maintaining nearly identical iteration counts and residual norms. Notably, even for this larger problem, the pattern holds that increasing the sketch size generally improves efficiency, with $\ell = 100$ providing the best performance. The residuals for RGl-GMRES are comparable to (and in some cases slightly better than) those obtained with Gl-GMRES, confirming that the randomized approach preserves accuracy while dramatically improving computational efficiency. When considered alongside the previous results, this table demonstrates that RGl-GMRES scales effectively to both larger problem dimensions ($l = 8$ vs. $l = 7$) and larger numbers of right-hand sides. The consistent performance gains across varying problem scales underscore the robustness and practicality of the randomized global approach for large-scale linear systems with multiple right-hand sides.

5. Conclusion

We have introduced a new randomized global GMRES method (RGl-GMRES) method for solving large-scale linear systems with multiple right-hand sides. The proposed approach combines global Krylov subspace techniques with randomized sketching to reduce computational cost and memory requirements, while preserving reliable convergence and accuracy. The numerical experiments conducted in Section 4 clearly demonstrate the efficiency and scalability of RGl-GMRES method. Compared to the standard Gl-GMRES method, the randomized variant achieves significant reductions in CPU time—in many cases by nearly 50%—without compromising solution quality. The performance gains become increasingly pronounced as the number of right-hand sides grows, confirming the method’s suitability for large-scale problems of the form (2). These results establish RGl-GMRES method as a practical, efficient, and robust solver

for high-dimensional multiple right-hand sides linear systems, offering a compelling alternative to classical deterministic approaches. Finally, the proposed randomized global framework naturally opens the door to further extensions. In particular, adapting the RGI-GMRES methodology to the solution of matrix equations such as Sylvester, Lyapunov, or more general linear matrix equations represents a promising direction for future research. By exploiting the intrinsic block and low-rank structures of these problems, randomized global Krylov techniques may lead to similarly significant reductions in computational complexity and memory usage, while maintaining accuracy and convergence robustness.

References

- [1] W.E. Arnoldi, The principle of minimized iterations in the solution of the matrix eigenvalue problem, *Quart. Appl. Math.*, 9 (1951), pp. 17-29.
- [2] O. Balabanov and L. Grigori, Randomized Gram-Schmidt process with application to GMRES, *SIAM J. Sci. Comput.*, 44 (2022), pp. A1450-A1474.
- [3] A. Badahmane, A.H. Bentbib and H. Sadok, Preconditioned global Krylov subspace methods for solving saddle point problems with multiple right-hand sides, *Electron. Trans. Numer. Anal.*, 51 (2019), pp. 495-511.
- [4] A. Badahmane, Regularized preconditioned gmres and the regularized iteration method, *Appl. Numer. Math.*, 152 (2020), pp. 159-168.
- [5] A. Badahmane, A.H. Bentbib and H. Sadok, Preconditioned global Krylov subspace methods for solving saddle point problems with multiple right-hand sides, *Electron. Trans. Numer. Anal.*, 51 (2019), pp. 495-511.
- [6] A. Badahmane, A. Ratnani, H. Sadok, Global accelerated Hermitian and skew-Hermitian splitting preconditioner for the solution of discrete Stokes problems. *J. Comput. Appl. Math.*, 468 (2025), pp. 116620.
- [7] A. Badahmane, Linear System Solutions of the Navier-Stokes Equations with Application to Flow over a Backward-Facing Step, *Open J. Fluid Dyn.*, 13 (2023), pp. 1-14.
- [8] M. BELLALIJ, K. JBILOU, AND H. SADOK, New convergence results on the global GMRES method for diagonalizable matrices, *J. Comput. Appl. Math.*, 219 (2008), pp. 350-358.
- [9] J.H. Bramble, J.E. Pasciak and A.T. Vassilev, Analysis of the inexact Uzawa algorithm for saddle point problems. *SIAM J. Numer. Anal.*, 34 (1997), pp. 1072-1092.

- [10] Y. Cao, J. Du, Q. Niu, Shift-splitting preconditioners for saddle point problems, *J. Comput. Appl. Math.*, 272 (2014), pp. 239-250.
- [11] A. Cortinovis, D. Kressner, and Y. Nakatsukasa, Speeding up Krylov subspace methods for computing ℓ_∞ norms via randomization, *SIAM J. Matrix Anal. Appl.*, 45 (2024), pp. 619-633.
- [12] H.C. Elman, D.J. Silvester, A.J. Wathen, *Finite Elements and Fast Iterative Solvers: with Applications in Incompressible Fluid Dynamics*, Oxford University Press, Oxford, UK., (2005).
- [13] J. Erhel, K. Burrage, B. Pohl, Restarted GMRES preconditioned by deflation, *J. Comput. Appl. Math.*, 69 (1996), pp. 303-318.
- [14] P. Guo, C.-X. Li and S.-L. Wu, A modified SOR-like method for the augmented systems, *J. Comput. Appl. Math.*, 274 (2015), pp. 58-69.
- [15] Z.-G. Huang, L.-G. Wang, Z. Xu, J.-J. Cui, A generalized variant of the deteriorated PSS preconditioner for nonsymmetric saddle point problems, *Numer. Algorithms*, 75 (2017), pp. 1161-1191.
- [16] K. JBILOU, A. MESSAOUDI, AND H. SADOK, Global FOM and GMRES algorithms for matrix equations, *Appl. Numer. Math.*, 31 (1999), pp. 49-63.
- [17] K. Jbilou, H. Sadok, A. Tinaztepe, Oblique projection methods for linear systems with multiple right-hand sides, *Electron. Trans. Numer. Anal.*, 20 (2005), pp. 119-138.
- [18] Z.-Z. Liang, G.-F. Zhang, Semi-convergence analysis of preconditioned deteriorated PSS iteration method for singular saddle point problems, *Numer. Algorithms*, 78 (2018), pp. 379-404.
- [19] P.-G. Martinsson and J. A. Tropp, Randomized numerical linear algebra: Foundations and algorithms, *Acta Numer.*, 29 (2020), pp. 403-572.
- [20] M. Meier, Y. Nakatsukasa, A. Townsend, and M. Webb, Are sketch-and-precondition least squares solvers numerically stable, *SIAM J. Matrix Anal. Appl.*, 45 (2024), pp. 905-929.
- [21] C. Musco and C. Musco, Randomized block Krylov methods for stronger and faster approximate singular value decomposition, *Adv. Neural Inf. Process. Syst.*, 28 (2015), pp. 1396-1404.
- [22] Y. Nakatsukasa and J. A. Tropp, Fast and accurate randomized algorithms for linear systems and eigenvalue problems, *SIAM J. Matrix Anal. Appl.*, 45 (2024), pp. 1183-1214.

- [23] Y. Saad, M.H. Schultz, GMRES: A generalized minimal residual algorithm for solving nonsymmetric linear systems, *SIAM J. Sci. Stat. Comput.*, 7 (1986), pp. 856-869.
- [24] Y. Saad, *Iterative Methods for Sparse Linear Systems*, SIAM, Philadelphia, PA, 2nd edition., (2003).
- [25] R. Bouyouli, G. Meurant, L. Smoch, H. Sadok, New results on the convergence of the conjugate gradient method, *Numer. Linear Algebra Appl.*, 16 (2009), pp. 223-236.
- [26] J. A. Tropp, Randomized block Krylov methods for approximating extreme eigenvalues, *Numer. Math.*, 150 (2022), pp. 217-255.
- [27] R. Vasav, T. Jourdan, G. Adjane, A. Badahmane, J. Creuze, M. Athènes, Cluster dynamics simulations using stochastic algorithms with logarithmic complexity in number of reactions, *J. Comput. Phys.*, 541 (2025), pp. 114318.
- [28] N.-N. Wang and J.-C. Li, A class of new extended shift-splitting preconditioners for saddle point problems, *J. Comput. Appl. Math.*, 357 (2019), pp. 123-145.
- [29] D. P. Woodruff, Sketching as a tool for numerical linear algebra, *Found. Trends Theor. Comput. Sci.*, 10 (2014), pp. 1-157.
- [30] J.-J. Zhang and J.-J. Shang, A class of Uzawa-SOR methods for saddle point problems, *Appl. Math. Comput.*, 216 (2010), pp. 2163-2168.
- [31] B. Zheng, Z.-Z. Bai and X. Yang, On semi-convergence of parameterized Uzawa methods for singular saddle point problems, *Linear Algebra Appl.*, 431 (2009), pp. 808-817.